Pergamon

Bioorganic & Medicinal Chemistry 9 (2001) 1155–1163

BIOORGANIC & MEDICINAL CHEMISTRY

Coupling between Substrate Binding and Allosteric Regulation in Ribozyme Catalysis

Michihiro Araki, Mie Hashima, Yasushi Okuno and Yukio Sugiura*

Institute for Chemical Research, Kyoto University, Uji, Kyoto 611-0011, Japan

Received 10 October 2000; accepted 2 December 2000

Abstract—The contribution of substrate binding to allosteric regulation in the ribozyme catalysis has been investigated using allosteric ribozymes consisting of the hammerhead ribozyme and a flavin mononucleotide (FMN) aptamer. Kinetic parameters were measured for various lengths of the substrates with a wide range of binding energy. The maximum cleavage rate of each ribozyme was retained with the long substrates. However, the cleavage rates largely decreased by the truncation of the substrates according to loss in the free energy of substrate binding. The high sensitivity to the substrate lengths is attributed to the increase in the energetic requirement for the catalytic core folding, which is caused by the incorporation of the aptamer region. One role of FMN binding is assisting the promotion of the core folding through the stabilization of the aptamer domain. The allosteric effect is significantly expressed only when the substrate binding energy is insufficient for the core folding of the ribozyme–substrate complex. This type of allosteric interaction dominates the substrate dependency of another type of regulation. These results demonstrate that an adequate correlation between the type of regulation and the substrate binding is responsible for the effective allosteric interaction in the kinetic process.

Introduction

The functional control observed in enzymatic catalysis is often attained by allosteric regulation, in which an allosteric effector binds to a part of an enzyme apart from its catalytic site and controls the catalytic activity.[1–8] The successful design of the allosteric interactions created the allosteric ribozymes by rational design and in vitro selection.[9–12] These ribozymes consisted of a ribozyme domain and a ligand binding site. The catalytic activities are regulated by small molecules, such as ATP, flavin mononucleotide (FMN) and theophylline. To achieve effective allosteric regulation, one must consider the entire interaction involved in the system, such as binding of ligand, binding of substrate, conformational state of the complex and rate constants for the various processes. There has been substantial evidence for the ligand binding, the conformational transition and the kinetics.[9–12] However, little is known about the connection between the role of the substrate binding in the enzymatic catalysis and the allosteric effect. We now ask if modulation of a substrate binding can affect the allosteric interactions in the kinetic process. For this purpose, we have introduced a simple allosteric regulatory system with a heterotropical interaction in a monomeric ribozyme.

To regulate the kinetic process by heterotropic interactions, not only the role of an allosteric effector but also the role of substrate binding in catalysis must be considered. Catalytic reaction is caused by stabilization of the transition state without equivalent stabilization of the ground state.[13] Enzymes have the ability to use energetic contribution in substrate binding interactions, which result in the alteration from the ground state to the transition state.[14,15] Therefore, substrate binding can prompt a conformational change from one to another state of an enzyme in a rate process. From this point of view, modulation of the substrate binding may alter the intrinsic equilibrium between the states to affect the kinetic regulation of enzymatic catalysis. Our previous study showed that a ribozyme with allosteric interaction could be constructed by unifying the hammerhead ribozyme as a catalytic site and a FMN aptamer as a regulatory site into a monomeric allosteric ribozyme (Fig. 1).[12] Binding of FMN to the aptamer domain promotes formation of the stem II region to regulate the catalytic reaction. In this allosteric ribozyme system, we could easily manipulate the substrate depending on the length and sequence of the helices. To

*Corresponding author. Tel.: +81-774-38-3210; fax: +81-774-32-3038; e-mail: sugiura@scl.kyoto-u.ac.jp

0968-0896/01/$ - see front matter
PII: S0968-0896(00)00336-9

evaluate coupling between the substrate binding and the kinetic control in the allosteric interactions, the contribution of the substrate binding to the kinetic property and the FMN effect in each ribozyme were measured using a series of substrates. The results show that the kinetic cooperativity is significantly dependent on the energetic contribution of the substrate binding.

Results and Discussion

Unusual sensitivity of intrinsic kinetic property to truncation of substrate

The hammerhead ribozyme can specifically cleave the substrate in an enzymatic catalysis manner.[16–19] The catalytic activity depends on proper folding in the conserved core of the internal loop region surrounded by three stem regions. The stems III and I are formed with the substrate, and the exact orientation of the stem II domain is important for the catalytic activity.[20–24] The allosteric ribozyme was constructed by incorporation of the FMN aptamer into the loop II region (Fig. 1).[12,25–28] Previous results indicated that the introduction of the aptamer region perturbed only the ribozyme with the unstable stem II region (<3 base pairs) to yield the conformational differences between the open and closed states. This structural equilibrium is the origin of the kinetic regulation by FMN. Specific FMN binding could assist the stem II formation and promote the subsequent core folding to enhance the cleavage rate. In the current study, the allosteric ribozymes with the unstable stem II (FR3M, 3AU and 2) were constructed to examine the substrate dependency of the allosteric regulation because it is predicted that the lower the stability of the stem II region, the more the effect of FMN.

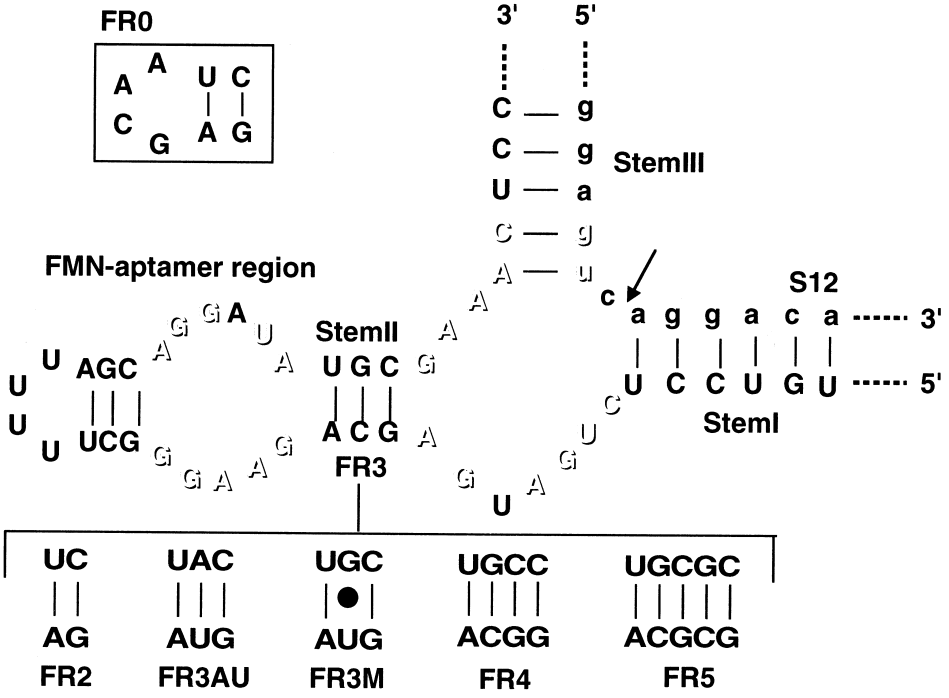

Figure 1. Designed allosteric ribozyme consisting of the core region of the hammerhead ribozyme and the FMN-binding aptamer region is depicted with the bound substrate, S12. The stems I and III recognize the substrate through base pairing with each other. The arrow indicates the position of cleavage. The outlined residues are essential to the catalytic activity of the hammerhead ribozyme (right) and the binding of FMN (left). Each construct includes different base pairs in the stem II region. FR0 has the stem II region identical to FR2 and GCAA loop instead of FMN–aptamer domain (boxed region).

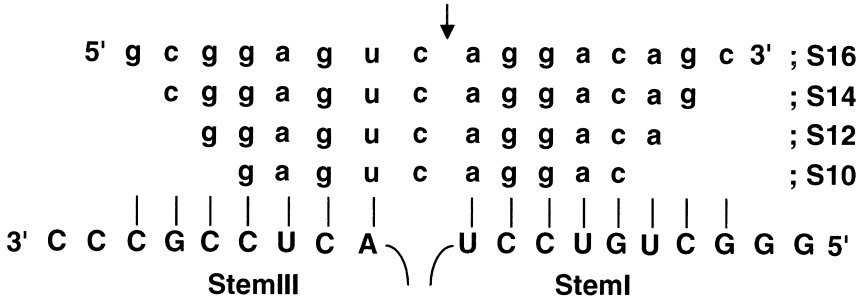

Figure 2. Illustration of various lengths of substrates with an extended version of the stems I and III. The arrow indicates the position of cleavage. The substrate sequences (top) are shown pairing to stems I and III on the ribozyme (bottom).

A series of substrates with various lengths were synthesized, based on the fact that the substrate binding affinity varies with the length of the substrate (Fig. 2).[29–31] Both stems I and III of the ribozyme were extended to be able to form helices with all substrates. To determine the individual effects of substrates on the kinetic property, the reaction rates were measured at varying ribozyme concentrations. The k_{obs} values of each reaction increase with increasing amounts of ribozyme concentration (Figs 3 and 4: open symbols). The maximum rates of each reaction at high ribozyme concentration depend on the substrate length. The observed rate constants of each reaction were fitted using a standard curve from the pseudo-first-order reaction. Table 1 summarizes the k_2 and K_m values of FR3M, FR3AU, and FR2. The k_2 values of all ribozymes with S14 and S16 showed similar values to that of FR0 (Table 2). On the other hand, the k_2 values observed in S10 significantly diminished by 10–10^3 times those observed in the reactions with S14 and S16. The decrease in the k_2 values was accompanied by an increase in the K_m values. In the case of FR0, only the K_m values respond to such a truncation of substrates (Table 2). Similar events were observed in the allosteric ribozymes with stable >4 base pairs in stem II (FR4 and 5, data not shown). It is thus suggested that the high sensitivity of the k_2 values to the substrate truncation is caused by the introduction of the FMN aptamer perturbing the stem II formation.

The single turnover experiments revealed that the intrinsic catalytic rate is highly dependent on the various lengths of the substrates. We next set out to determine the affinity for the ribozyme-substrate complexes to explore the energetic contribution of substrate binding to each cleavage rate. If the equilibration between the bound and unbound substrates is fast compared to the cleavage, the K_m values correspond to K_d values. However, the cleavage reaction should be fast under the present experimental condition because the cleavage

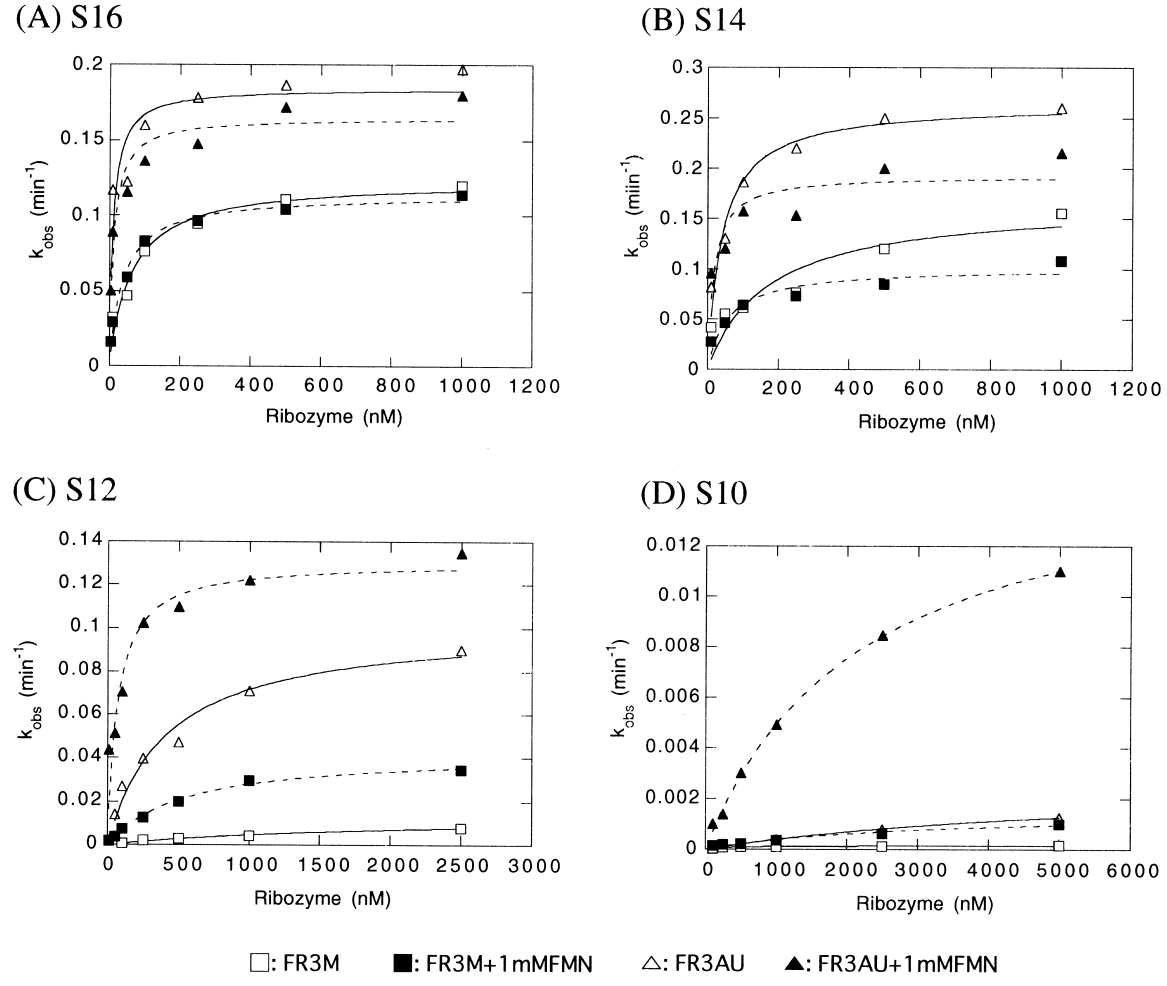

Figure 3. Determination of kinetic parameters for a series of substrates and FR3M and 3AU. Representative rate versus ribozyme concentration plots are shown. The k_{obs} values were obtained by single-turnover experiments. Values of k_2 and K_m were determined by plotting the k_{obs} values as a function of the ribozyme concentration and fitting the plot to eq (1) (see Materials and Methods). The open symbols and solid line represent data from the reaction without 1 mM FMN. The closed symbols and dashed line indicate data from the reaction with 1 mM FMN. All of the kinetic parameters are summarized in Table 1. (A) Kinetic behavior of FR3M (square) and FR3AU (triangle) toward S16 in the absence and presence of 1 mM FMN. Reactions were performed with various concentrations (1 nM∼1 μM) of each ribozyme. (B) Kinetic behavior of each ribozyme toward S14. Reactions were performed with the various concentrations (1 nM∼1 μM) of each ribozyme. (C) Kinetic behavior of each ribozyme toward S12. Reactions were performed with various concentrations (10 nM∼2.5 μM) of each ribozyme. (D) Kinetic behavior of each ribozyme toward S10. Reactions were performed with various concentrations (100 nM∼5 μM) of each ribozyme.

rates were extremely slow in the reaction with S10. In this condition, the equilibrium between the bound and unbound substrates was not suggested to be faster than the cleavage rate. Therefore, we performed pulse-chase experiments to evaluate the k_{-1} values in all cases. A typical example (FR3M-S16) is shown in Figure 5. In the reactions with S10 and S12, the equilibration rates between the bound and unbound substrates exceeded the cleavage rates, and the K_d values were very close to the K_m values (Table 1). The binding energy of the substrates was calculated using K_d values ($\Delta G_{bind} = -RT\ln(1/K_d)$) (see Experimenal). The K_d values varied over a wide range according to the length of substrates, as observed in the K_m values. Compared with FR0, these values were 10^2–10^3 times higher, and the free energy of the substrate binding showed lower values. The decrease in the substrate binding energy may be due to the deformation of the stem II region. However, the loss in the substrate binding energy cannot directly account for the decrease in the cleavage rate to the substrate deletion, because the maximum k_2 values of each ribozyme indicated similar values to that of FR0. Correlation between the k_2 values and the substrate binding energy revealed that the k_2 values of each ribozyme almost correspond to those of FR0 in reaction with the long substrates of nearly 10 kcal/mol of binding energy. This value is higher than the unfavorable free energy of $\Delta G_{core} \approx +3$–$7$ kcal/mol for folding of the hammerhead core.[32–34] The high sensitivity of the k_2 values to the substrate deletion is attributed to the increase in the unfavorable energy of the core folding. Why does the deformation of the stem II region give rise to the unfavorable energy? There is substantial evidence for a conformational change prior to the cleavage of a bound substrate by the hammerhead ribozyme.[35–41] Several base residues and functional groups play a crucial role in this process, despite the fact that they have no structural connections to the cleavage site. The formation of the stem II region is also one of the connections participating in the core folding. Thus, the

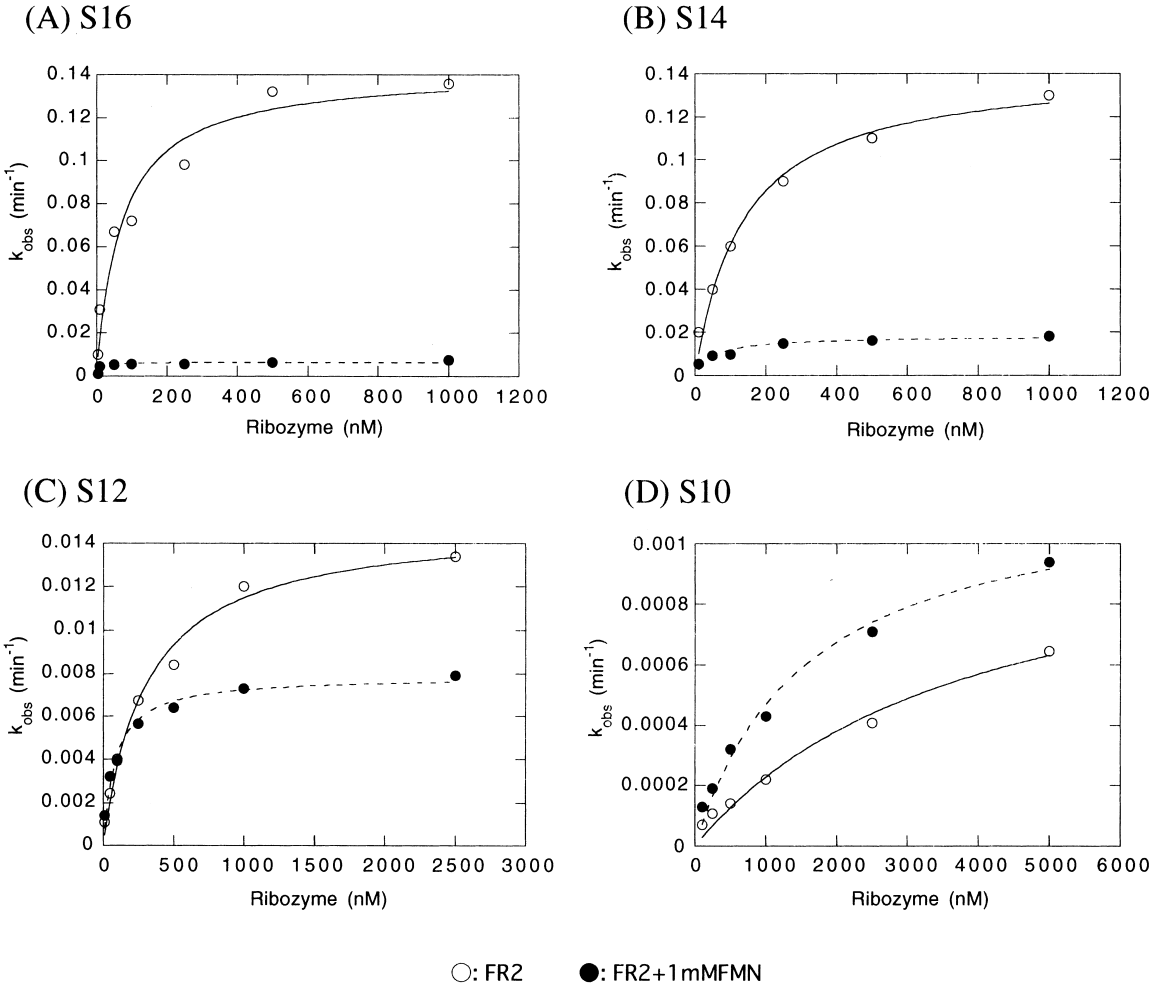

Figure 4. Determination of kinetic parameters for a series of substrates and FR2. Representative rate versus ribozyme concentration plots are shown. The k_{obs} values were obtained by single-turnover experiments. Values of k_2 and K_m were determined by plotting the k_{obs} values as a function of the ribozyme concentration and fitting the plot to eq (1) (see Materials and Methods). The open symbols and solid line represent data from the reaction without 1 mM FMN. The closed symbols and dashed line indicate data from the reaction with 1 mM FMN. All of the kinetic parameters are summarized in Table 1. (A) Kinetic behavior of FR2 (circle) toward S16 in the absence and presence of 1 mM FMN. Reactions were performed with various concentrations (1 nM~1 μM) of each ribozyme. (B) Kinetic behavior of each ribozyme toward S14. Reactions were performed with various concentrations (1 nM~1 μM) of each ribozyme. (C) Kinetic behavior of each ribozyme toward S12. Reactions were performed with various concentrations (10 nM~2.5 μM) of each ribozyme. (D) Kinetic behavior of each ribozyme toward S10. Reactions were performed with various concentrations (100 nM~5 μM) of each ribozyme.

deformation of the stem II domain increases the energetic requirement for the core folding to yield the conformational equilibrium.

Coupling between substrate binding and kinetic regulation by FMN

The single turnover experiments with FR3M, FR3AU, and FR2 to S10–16 were performed in the presence of 1 mM FMN to evaluate the substrate dependency of the allosteric regulation by FMN (closed symbols in Figs 3 and 4). The k_{obs} values of each reaction are dependent on the ribozyme concentration as observed in the reaction without FMN. Each maximum rate at high ribozyme–FMN complex concentration varies according to the substrate length except for that of the FR2–FMN complex (see below). The dissociation constants for the substrate binding in the presence of excess FMN were also determined by the pulse-chase experiment (Fig. 5). As shown in Table 1, the k_2 values of FR3M and FR3AU were enhanced by about 10-fold in the case of the reaction with S10 or S12, while the k_2 values to S14 and S16 were almost unchanged. There are no remarkable effects on the K_d values. The k_2 values of

Table 1. Kinetic parameters for FR3M, FR3AU, and FR2 to each substrate with and without 1 mM FMN[a]

Substrate	FMN (mM)	k_2 (min^{-1})	K_m (nM)	K_d (nM)[b]	ΔG_{bind} (kcal/mol)[c]
FR3M					
S10	—	$(1.6\pm0.12)\times10^{-4}$	3900±1200	2300	−8.0
S12	—	$(4.2\pm0.51)\times10^{-3}$	590±65	240	−9.4
S14	—	$(1.4\pm0.33)\times10^{-1}$	170±100	34	−10.6
S16	—	$(1.3\pm0.02)\times10^{-1}$	40±4	10	−11.4
S10	1	$(1.5\pm0.33)\times10^{-3}$	3000±1300	1800	−8.2
S12	1	$(3.5\pm0.29)\times10^{-2}$	580±92	120	−9.8
S14	1	$(1.0\pm0.09)\times10^{-1}$	58±22	12	−11.3
S16	1	$(1.2\pm0.03)\times10^{-1}$	27±3	9	−11.4
FR3AU					
S10	—	$(2.8\pm0.04)\times10^{-3}$	3000±1600	1200	−8.4
S12	—	$(1.0\pm0.28)\times10^{-3}$	200±90	36	−10.6
S14	—	$(2.5\pm0.25)\times10^{-1}$	51±19	10	−11.3
S16	—	$(2.0\pm0.11)\times10^{-1}$	12±4	2.4	−12.2
S10	1	$(1.3\pm0.22)\times10^{-2}$	2200±740	850	−8.6
S12	1	$(1.3\pm0.10)\times10^{-1}$	56±13	15	−11.1
S14	1	$(1.9\pm1.17)\times10^{-1}$	18±10	4	−11.9
S16	1	$(1.9\pm0.10)\times10^{-1}$	16±4	2.3	−12.3
FR2					
S10	—	$(1.1\pm0.20)\times10^{-3}$	3900±650	2700	−7.9
S12	—	$(1.5\pm0.14)\times10^{-2}$	301±73	167	−9.6
S14	—	$(1.3\pm0.21)\times10^{-1}$	212±47	77	−10.1
S16	—	$(1.4\pm0.28)\times10^{-1}$	74±19	7.4	−11.5
S10	1	$(1.2\pm0.09)\times10^{-3}$	1600±310	1100	−8.4
S12	1	$(7.9\pm0.30)\times10^{-3}$	86±14	57	−10.3
S14	1	$(8.5\pm0.14)\times10^{-3}$	55±19	28	−10.7
S16	1	$(6.9\pm0.60)\times10^{-3}$	8±6	1.6	−12.4

[a]The k_2 and K_m values were obtained by monitoring the pseudo-first-order, single-turnover reaction rates as a function of ribozyme concentration (see Figs 3 and 4). Errors were obtained from the fits to the data. Reactions were performed at 37 °C in a buffer of 50 mM Tris–HCl (pH 7.5), 5 mM $MgCl_2$, and 50 mM NaCl.
[b]Values of $K_d(k_{-1}/k_1)$ were calculated from values of k_2, K_m, and k_{-1}.
[c]Binding free energies were determined from the relationsip $\Delta G_{bind} = -RTln(1/K_d)$, where T is 310 K and R is 0.001987 kcal/mol/K for each substrate.

Table 2. Kinetic parameters for FR0 to each substrate with and without 1 mM FMN[a]

Substrate	FMN (mM)	k_2 (min^{-1})	K_m (nM)	K_d (nM)[b]	ΔG_{bind} (kcal/mol)[c]
S10	—	$(1.9\pm0.12)\times10^{-3}$	510±120	70	−10.1
S12	—	$(4.2\pm0.51)\times10^{-1}$	110±65	5	−11.8
S14	—	$(5.1\pm0.33)\times10^{-1}$	17±10	0.03	−14.9
S16	—	$(5.3\pm0.02)\times10^{-1}$	3±1	0.002	−16.6
S10	1	$(1.8\pm0.33)\times10^{-1}$	730±130	110	−9.9
S12	1	$(3.5\pm0.29)\times10^{-1}$	170±92	11	−11.3
S14	1	$(4.6\pm0.09)\times10^{-1}$	25±12	0.1	−14.2
S16	1	$(5.0\pm0.03)\times10^{-1}$	5±3	0.008	−15.7

[a]The k_2 and K_m values were obtained by monitoring the pseudo-first-order, single-turnover reaction rates as a function of ribozyme concentration (see Figs 3 and 4). Errors were obtained from the fits to the data. Reactions were performed at 37 °C in a buffer of 50 mM Tris–HCl (pH 7.5), 5 mM $MgCl_2$, and 50 mM NaCl.
[b]Values of $K_d(k_{-1}/k_1)$ were calculated from values of k_2, K_m, and k_{-1}.
[c]Binding free energies were determined from the relationship $\Delta G_{bind} = -RTln(1/K_d)$, where T is 310 K and R is 0.001987 kcal/mol/K for each substrate.

FR3M and FR3AU–FMN complexes were dependent on the substrate sequences, as can be observed in the reaction without FMN. From these facts, FMN assists the folding of the unfolded catalytic core rather than the substrate binding. These results are consistent with the previous results where specific FMN binding could rescue the stem II formation and promote the subsequent core folding to enhance the cleavage rate. In this sense, FMN binding on FR3M and FR3AU has the same effect on the catalytic rate as the energetic contribution of the substrate binding. The common effects on the catalytic rate lead to the substrate dependency of the FMN regulation. A marked effect is expressed only when the ratio of the open complex exceeds that of the closed state, as shown in the reaction with the short substrates.

The effects of FMN on FR2 provided another example for the substrate dependency of the allosteric regulation. Remarkable inhibition of the cleavage rate by FMN was observed in the reaction with the long substrates (Table 1). The structural basis for the inhibition of the k_2 value is explained by the superimposition of the atomic coordinates of the hammerhead ribozyme and the FMN aptamer (data not shown).[27,35–38] The structure of the FMN aptamer reveals that the loop region folds compactly and forms an approximately A-form helical structure, except that the adenine residue sticks out upon FMN binding. By the fusion of this aptamer domain to the hammerhead ribozyme, the adenine residue is arranged to impair the catalytic core only in stem II of the two base pairs, FR2. However, the inhibitory effect could not be observed in the reaction with S10. The low k_2 values of the FR2–FMN complex were independent of the substrate with a wide range of binding energy. These results suggest that FMN would regulate the cleavage rate of FR2 in two opposite ways, the inhibition of the cleavage chemistry and the promotion of the core folding. In the case of the long substrates, only the inhibitory effect expresses as output from FMN binding because FMN has no effect on the core folding. No remarkable effect was observed in the short substrate, which is attributed to the inhibitory effect being offset by the core folding effect. This type of regulation is thus

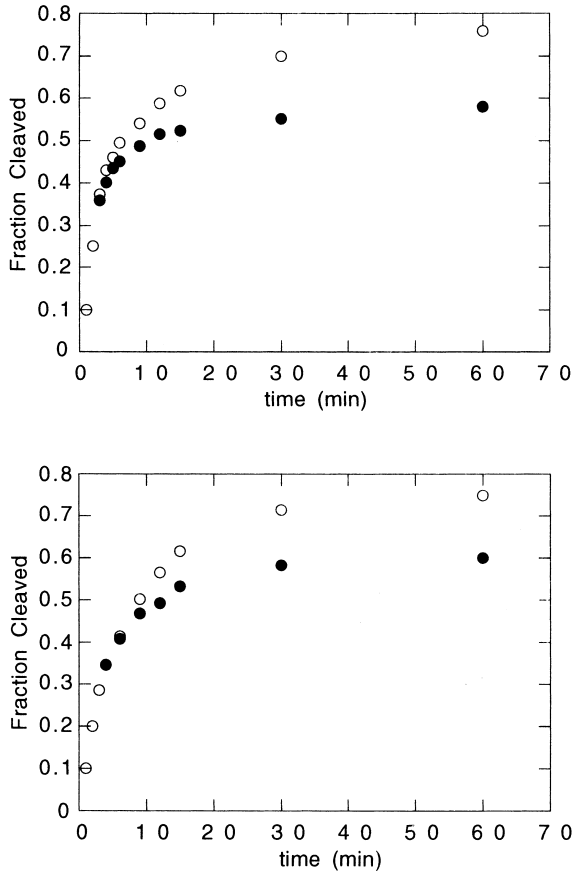

Figure 5. Pulse-chase experiments for FR3M-S16 to determine substrate dissociation rate constants. The fraction of substrate converted to product at various times is shown for a reaction in which 1 μM FR3M was combined with a trace amount of [5′-^{32}P] S16 in the absence (upper) and presence (lower) of 1 mM FMN. After 3 min, t_1, the reactions were chased with 25 μM nonradioactive S16 (●), or the reaction was allowed to proceed without the chase (○).

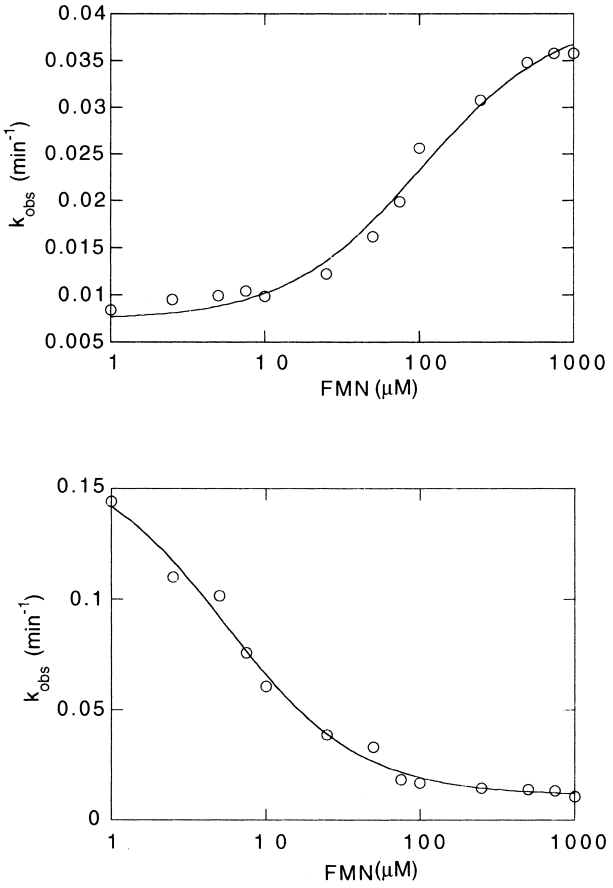

Figure 6. FMN concentration dependence of the observed first-order rates. Single-turnover reactions after pre-annealing were carried out at increasing concentrations of FMN. (Upper) FMN dependent enhancement of the observed rate of FR3M–S12 complex. The reactions were performed with 2.5 μM FR3M and a trace amount of S12 at various concentrations of FMN. The line indicates the least squares fits of the experimental data to eq (2). (Lower) FMN dependent inhibition of the observed rate of the FR2–S16 complex. The reactions were performed with 1 μM FR2 and a trace amount of S16 at various concentrations of FMN. The line indicates the least squares fits of the experimental data to eq (2).

distinctly expressed when the catalytic core is fully folded, as observed in the reaction with S16.

Different effect of specific FMN binding on each ribozyme

To evaluate two effects of FMN binding on the cleavage rate, the reaction rates for FR3M–S12 and FR2–S16 complexes were plotted as a function of FMN concentration (Fig. 6). These conditions were chosen because the FMN effect on the ribozyme is remarkably exhibited in each case. The marked dependence on the FMN binding for both ribozymes indicated that specific binding of FMN to the aptamer region regulated the cleavage rate. The dissociation constants of FMN from the FR3M and FR2–substrate complex were estimated to be 140 and 6 μM, respectively. The difference between each K_{dF} value may be attributed to the state difference (open or closed) in the stem II region. These results strongly support the idea that FMN binds to the open state of FR3M with low affinity to promote the core folding, and FMN binds to the closed state of FR2 with high affinity to inhibit the cleavage chemistry. The lower K_{dF} value is in good agreement with the apparent K_d values obtained for similar allosteric ribozymes that were in vitro selected by modulating the stem II region.[39–41] This correspondence suggests that the in vitro selected ribozyme would exist as the closed state, and would not take the energetic contribution of the substrate binding into account. By manipulating the substrate sequences, it is possible to create the allosteric ribozyme under more effective regulation.

Conclusion

By measuring the substrate dependency of the allosteric regulation, we have demonstrated the relation between the allosteric regulation and the contribution of the substrate binding to the catalytic rate. One role of FMN is assisting in the core folding through the stem II formation. This effect is mainly due to the energetic contribution of the substrate binding and determines the substrate dependency of the allosteric regulation. Another role is the effect on the cleavage chemistry in the reaction. This effect itself is independent of the substrate binding. However, the substrate dependency of the allosteric regulation is dominated by the core folding effect. These observations demonstrate that modulation of the substrate binding alters the intrinsic equilibrium balance in the catalytic process to affect the allosteric interactions. The connection between the substrate binding and the allosteric regulation is an essential factor to achieve effective allosteric regulation.

Experimental

RNA preparations

All synthetic DNAs were purchased from Amersham Pharmacia Biotech. Double-stranded templates of ribozymes were constructed by a polymerase chain reaction using the corresponding antisense DNA and the primers. Each ribozyme was prepared by in vitro transcription from the DNA template using T7 RNA polymerase as previously described.[12,42] RNA was purified by electrophoresis through a 15% denaturing polyacrylamide gel electrophoresis (PAGE), staining in ethidium bromide solution, visualized by UV, excised, and eluted overnight at room temperature in 500 mM ammonium acetate solution containing 1 mM EDTA. The eluates were extracted with 1-butanol, and then ethanol-precipitated. RNA pellets were washed with 70% ethanol, dried, resuspended in water, and quantified by measuring the absorbance at 260 nm. The RNA substrate was prepared by standard solid-phase methods.[43] Substrate RNA was purified by a 20% PAGE, 5′-^{32}P end-labeled with T4 polynucleotide kinase and [γ-^{32}p] ATP and was repurified by a 20% PAGE.

General kinetic analysis

Single turnover experiments were performed under the conditions of excess ribozyme (final concentration, 1 nM–10 μM) with the substrate (final concentration, ~0.5 nM). Ribozyme and substrate were separately denatured for 1 min at 70 °C in 50 mM Tris–HCl buffer (pH 7.5) containing 50 mM NaCl and cooled at room temperature for 15 min. Each sample solution containing 5 mM $MgCl_2$ was incubated at 37 °C for 15 min. The reactions were initiated by mixing two sample solutions at 37 °C. In certain cases, the ribozyme and substrate were heated and cooled in the buffer, and then the reaction was initiated by the addition of $MgCl_2$ to 5 mM concentration. Aliquots of the reaction mixture were removed at appropriate intervals and quenched with an equal volume of 100 mM Tris–HCl/100 mM boric acid/10 mM EDTA/9 M urea/0.1% xylene cyanol/0.1% bromophenol blue. To obtain the rate constants from the initial rates, the quenching interval was varied from 30 s to 10 h depending on the observed cleavage rate of each reaction. The extents of cleavage were analyzed by a 20% PAGE and detected by autoradiography. The simple two-step reaction pathway is described by the mechanism of the cleavage reaction as follows:

$$E + S \underset{k_{-1}}{\overset{k_1}{\rightleftharpoons}} E \cdot S \xrightarrow{k_2} \text{Products}$$

Scheme 1.

The time course of all reactions fitted well to a single-exponential function with end points of ~90%. Apparent cleavage rates (k_{obs}) were obtained from the slope of a semilogarithmic plot (logarithm of unreacted fraction versus time) derived from the pseudo-first-order reaction equation.[44–46] The k_{obs} values were evaluated from two or three independent experiments varying $< 20\%$. To determine the kinetic parameters for k_2 and K_m, the k_{obs} values were plotted as a function of the ribozyme concentration for each substrate. In each FMN-dependent experiment, the rate constant was determined similarly, except for the addition of 1 mM FMN during the incubation. Most of the ribozymes exist as the

FMN–ribozyme complex form and are regarded as E in Scheme 1 in this condition. The resulting apparent binding curves were fitted to a standard Michaelis–Menten curve (eq (1)).

$$k_{obs} = \frac{k_2 \cdot [E]}{K_m + [E]} \quad (1)$$

K_m is the Michaelis–Menten constant corresponding to $(k_2 + k_{-1})/k_1$. Curve fitting yields k_2 as the horizontal asymptote of the plot and K_m as the ribozyme concentration at half-maximal rate ($R^2 > 0.98$).

To determine the affinity of FMN for the ribozyme–substrate complex, the single-turnover experiments at constant ribozyme concentration over the radioactive substrate were performed with increasing concentrations of FMN. In these experiments, the ribozyme–substrate complexes were equilibrated before initiation of the reaction with a mixture of 5 mM $MgCl_2$ and various concentrations of FMN. The k_{obs} values were plotted as a function of the FMN concentration. Each plot of FR3M and FR2 was fitted to eq (2) derived as previously described.[12]

$$k_{obs} = \frac{k_{chem} \cdot K_{dF} + k'_{chem} \cdot F}{K_{dF} + F} \quad (2)$$

Determination of dissociation constants for ribozyme–substrate complex

The method for determining the thermodynamic dissociation constants of the enzyme–substrate complexes ($K_d = k_{-1}/k_1$) depends on the kinetic property of the individual ribozyme. Here, K_d values were determined using pulse-chase reaction under the same conditions as the cleavage reaction.[45,46] First, each ribozyme and a trace amount of radioactive substrate were combined at a sufficiently high concentration ranging from 10 to 100 times the K_m value. After an initial binding period, t_1, at 37 °C, excess amounts of a nonradioactive substrate were added to initiate the chase reaction. The duration of the initial binding period ranged from 1 to 30 min. The concentration of the nonradioactive substrate during the chase ranged from 50 to 100 times the ribozyme concentration. During the chase period, t_2, samples were removed at appropriate intervals and quenched. The t_2 value corresponds to 3 times the $t_{1/2}$ value for the cleavage reaction. The control reactions were performed similarly, except for the addition of the nonradioactive substrate. The samples were removed from the reaction after the initiation throughout the chase reaction. The substrates and products were quantitated as described in the single-turnover experiment. The rate constants for substrate dissociation (k_{-1}) were calculated by comparing the chase and control reactions at long times, as previously described.[46] The K_d ($= k_{-1}/k_1$) values were then calculated from the experimentally determined K_m, $(k_2 + k_{-1})/k_1$.

Acknowledgements

This study was supported in part by a Grant-in-Aid for Scientific Research from the Ministry of Education, Science, Sports and Culture, Japan. M.A. is a research fellow of the Japan Society for the Promotion of Science.

References

1. Monod, J.; Wyman, J.; Changeux, J. P. *J. Mol. Biol.* **1965**, *12*, 88.
2. Koshland, D. E.; Nemethy, G.; Filmer, D. *Biochemistry* **1966**, *5*, 365.
3. Neet, K. E. *Methods Enzymol.* **1995**, *249*, 519.
4. Ricard, J.; Cornish-Bowden, A. *Eur. J. Biochem.* **1987**, *166*, 255.
5. Goldbeter, A. *Biophys. Chem.* **1976**, *4*, 159.
6. Perutz, M. F. *Mechanisms of Cooperativity and Allosteric Regulation in Proteins*; Cambridge University Press: New York, 1994.
7. Ackers, G. K.; Doyle, M. L.; Myers, D.; Daugherty, M. A. *Science* **1992**, *255*, 54.
8. Fersht, A. *Enzyme Structure and Mechanism*; W. H. Freeman: New York, 1985.
9. Tang, J.; Breaker, R. R. *Chem. Biol.* **1997**, *4*, 453.
10. Soukup, G. A.; Breaker, R. R. *Structure* **1999**, *7*, 783.
11. Soukup, G. A.; Breaker, R. R. *Proc. Natl. Acad. Sci. U.S.A.* **1999**, *96*, 3584.
12. Araki, M.; Okuno, Y.; Hara, Y.; Sugiura, Y. *Nucleic Acids Res.* **1998**, *26*, 3379.
13. Lienhard, G. E. *Science* **1973**, *180*, 149.
14. Jencks, W. P. *Adv. Enzymol.* **1975**, *43*, 219.
15. Narlikar, G. J.; Herschlag, D. *Annu. Rev. Biochem.* **1997**, *66*, 19.
16. Uhlenbeck, O. C. *Nature* **1987**, *328*, 596.
17. Mckay, D. B. *RNA* **1996**, *2*, 395.
18. Haseloff, J.; Gerlach, W. L. *Nature* **1988**, *334*, 585.
19. Symons, R. H. *Annu. Rev. Biochem.* **1992**, *61*, 641.
20. Tuschl, T.; Eckstein, F. *Proc. Natl. Acad. Sci. U.S.A.* **1993**, *90*, 6991.
21. McCall, M. J.; Hendry, P.; Jennings, P. A. *Proc. Natl. Acad. Sci. U.S.A.* **1992**, *89*, 5710.
22. Fu, D.; Benseler, F.; Mclaughlin, L. W. *J. Am. Chem. Soc.* **1994**, *116*, 4591.
23. Peracchi, A.; Karpeisky, A.; Maloney, L.; Beigelman, L.; Herschlag, D. *Biochemistry* **1998**, *37*, 14765.
24. Peracchi, A.; Beigelman, L.; Scot, E. C.; Uhlenbeck, O. C.; Herschlag, D. *J. Biol. Chem.* **1997**, *272*, 26822.
25. Burgstaller, P.; Famulok, M. *Angew. Chem., Int. Ed. Engl.* **1994**, *33*, 1084.
26. Burgstaller, P.; Famulok, M. *Bioorg. Med. Chem. Lett.* **1996**, *6*, 1157.
27. Fan, P.; Suri, A. K.; Fiara, R.; Live, D.; Patel, D. J. *J. Mol. Biol.* **1996**, *258*, 480.
28. Patel, D. J.; Suri, A. K.; Jiang, F.; Jiang, L.; Ajay Kumar, P. F. R.; Nonin, S. *J. Mol. Biol.* **1997**, *272*, 645.
29. Freier, S. M.; Kierzek, R.; Jaeger, J. A.; Sugimoto, N.; Caruthers, M. H.; Neilson, T.; Turner, D. H. *Proc. Natl. Acad. Sci. U.S.A.* **1986**, *83*, 9373.
30. Hendry, P.; McCall, M. *Nucleic Acids Res.* **1996**, *24*, 2679.
31. Clouet-d'Orval, B.; Uhlenbeck, O. C. *Biochemistry* **1997**, *36*, 9087.
32. Hertel, K. J.; Stage-Zimmermann, T. K.; Ammons, G.; Uhlenbeck, O. C. *Biochemistry* **1998**, *37*, 16983.
33. Hertel, K. J.; Peracchi, A.; Uhlenbeck, O. C.; Herschlag, D. *Proc. Natl. Acad. Sci. U.S.A.* **1997**, *94*, 8497.

34. Hertel, K. J.; Herschlag, D.; Uhlenbeck, O. C. *EMBO J*. **1996**, *15*, 3751.
35. Pley, H. W.; Flaherty, K. M.; McKay, D. B. *Nature* **1994**, *372*, 68.
36. Scott, W. G.; Finch, J. T.; Klug, A. *Cell* **1995**, *81*, 991.
37. Scott, W. G.; Murray, J. B.; Arnold, J. R. P.; Stoddard, B. L.; Klug, A. *Science* **1996**, *274*, 2065.
38. Murray, J. B.; Terwey, D. P.; Maloney, L.; Karpeisky, A.; Usman, N.; Beigelman, L.; Scott, W. G. *Cell* **1998**, *92*, 665.
39. Feig, A. L.; Scott, W. G.; Uhlenbeck, O. C. *Science* **1998**, *279*, 81.
40. Bassi, G. S.; Murchie, A. I. H.; Walter, F.; Clegg, R. M.; Lilley, D. M. J. *EMBO J*. **1997**, *16*, 7481.
41. Bassi, G. S.; Mollegaard, N. E.; Murchie, A. I. H.; Kitzing, E. V.; Lilley, D. M. J. *Nat. Struct. Biol*. **1995**, *2*, 45.
42. Milligan, J. F.; Uhlenbeck, O. C. *Methods Enzymol*. **1989**, *180*, 51.
43. Wincott, F.; DiRenzo, A.; Shaffer, C.; Tracz, D.; Workman, C.; Sweedler, D.; Gonzales, C.; Scaringe, S.; Usman, N. *Nucleic Acids Res*. **1995**, *23*, 2677.
44. Ruffner, D. L.; Stormo, G. D.; Uhlenbeck, O. C. *Biochemistry* **1990**, *29*, 10695.
45. Fedor, M. J.; Uhlenbeck, O. C. *Biochemistry* **1992**, *31*, 12042.
46. Hertel, K. J.; Herschlag, D.; Uhlenbeck, O. C. *Biochemistry* **1994**, *33*, 3374.